

## Supporting information for

# Experimental visualization of lithium conduction pathways in Garnet-type $\text{Li}_7\text{La}_3\text{Zr}_2\text{O}_{12}$

Jiantao Han,<sup>a</sup> Jinlong Zhu,<sup>a</sup> Yutao Li,<sup>b</sup> Xiaohui Yu,<sup>a</sup> Shanmin Wang,<sup>a</sup> Gang Wu,<sup>a</sup> Hui Xie,<sup>b</sup> Sven C. Vogel,<sup>a</sup> Fujio Izumi,<sup>c</sup> Koichi Momma,<sup>d</sup> Yukihiko Kawamura,<sup>e</sup> Yunhui Huang,<sup>f</sup> John B. Goodenough,<sup>b</sup> Yusheng Zhao<sup>a</sup>

<sup>a</sup> LANSCE-Lujan Neutron Scattering Center, Los Alamos National Laboratory, Los Alamos, New Mexico, 87545

<sup>b</sup> Texas Materials Institute, ETC 9.102, the University of Texas at Austin, TX 78712, USA

<sup>c</sup> Quantum Beam Center, National Institute for Materials Science, Namiki, Tsukuba, Ibaraki 305-0044, Japan

<sup>d</sup> National Museum of Nature and Science, Tsukuba, Ibaraki 305-0005, Japan

<sup>e</sup> Research Center for Neutron Science and Technology, Tokai-mura, Naka-gun, Ibaraki 319-1106, Japan

<sup>f</sup> School of Materials Science and Engineering, Huazhong University of Science and Technology, Wuhan, Hubei 430074, China

## Experimental Section

Neutron diffraction includes some important information on lithium, because the scattering ability of the lithium nucleus is relatively large and independent of scattering vector  $Q = 4\pi\sin\theta/\lambda$ . This nature is amenable for detailed analysis of the thermal motion of the lithium nucleus, in contrast to the negligible X-ray scattering ability of lithium or lithium ions with only two or three electrons. To enhance this advantage,  ${}^7\text{Li}_7\text{La}_3\text{Zr}_2\text{O}_{12}$  was prepared using  ${}^7\text{Li}$  enriched  $\text{Li}_2\text{CO}_3$  as the raw material.  $\text{Li}_7\text{La}_3\text{Zr}_2\text{O}_{12}$  was prepared by solid-state reaction of stoichiometric amounts of  $\text{Li}_2\text{CO}_3$ ,  $\text{La}_2\text{O}_3$  (heated at  $900^\circ\text{C}$  for 12 h) and  $\text{ZrO}_2$ . 10 wt% excess  $\text{Li}_2\text{CO}_3$  was added to compensate for the loss of lithium during annealing. The powders were ground and heated to  $900^\circ\text{C}$  to decompose the metal salts. Finally, the powders were ground again, pressed into a pellet, and annealed at  $1120^\circ\text{C}$ ,  $1140^\circ\text{C}$ , and  $1230^\circ\text{C}$  while the pellet was covered with the same mother powder. The annealing was done in an alumina crucible.

Powder X-ray diffraction (Philips PW1830, Cu  $K\alpha$ ) was employed to monitor the phase formation in the  $2\theta$  range from  $10$  to  $70^\circ$  with a step size of  $0.02^\circ$ . The lattice parameters were calculated from the diffraction peaks in the range  $20$ - $60^\circ$  with Jade software. Neutron diffraction experiments were conducted on the high-pressure preferred orientation neutron diffractometer (HIPPO) at the Lujan Neutron Scattering Center, Los Alamos National Laboratory. Bulk samples were placed in a vanadium can and time-of-flight data were collected under vacuum. Neutrons were detected with 27 detector panels of  ${}^3\text{He}$  detector tubes arranged on three rings with nominal diffraction angles of  $40^\circ$ ,  $90^\circ$ , and  $144^\circ$ . The GSAS program was used to perform Rietveld refinement with background functions type 1 and 16 for background coefficients.

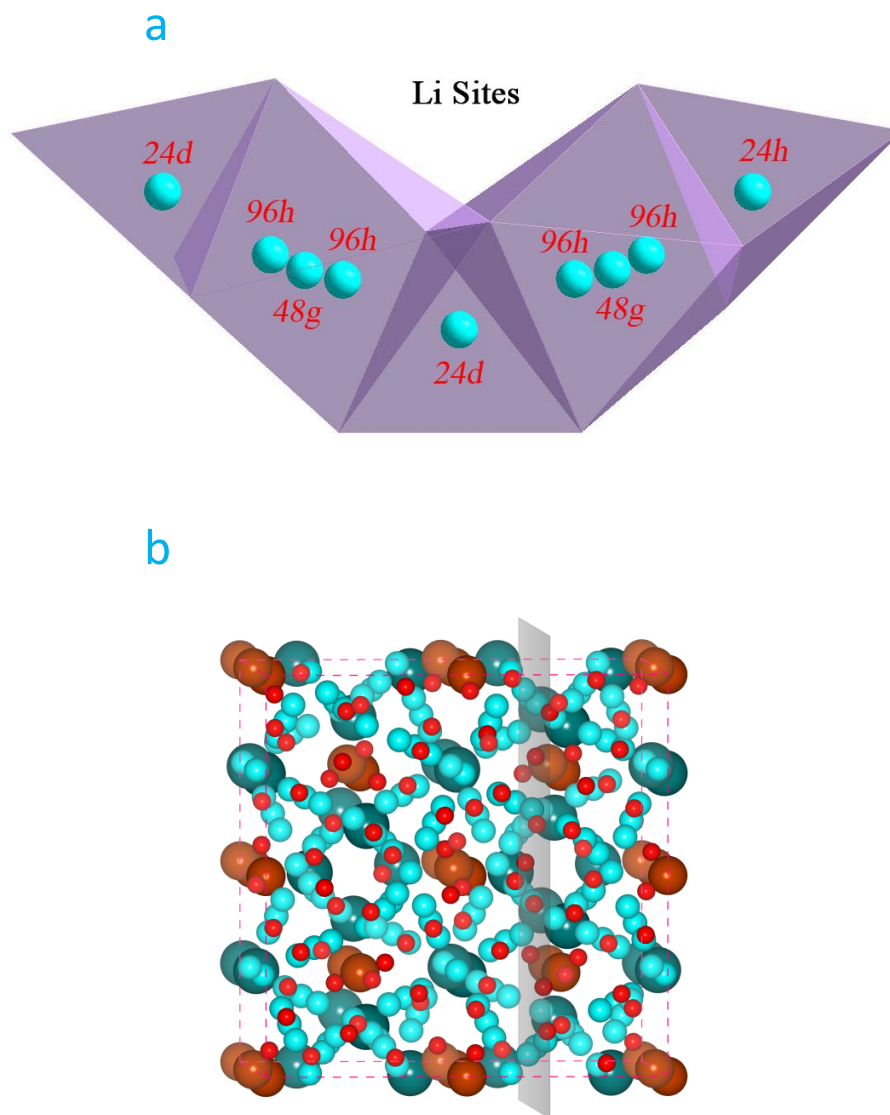


Figure S1. (a) The atomic structure of garnet-type *c*-LLZO, (b) Wyckoff positions that the Li ions could be located. The centers of Li(1), Li(2) and Li(3) sites are noted as *24d*, *48g* and *96h* sites, respectively, and the *96h* sites are slightly displaced off the *48g* sites but they are still inside the octahedra.

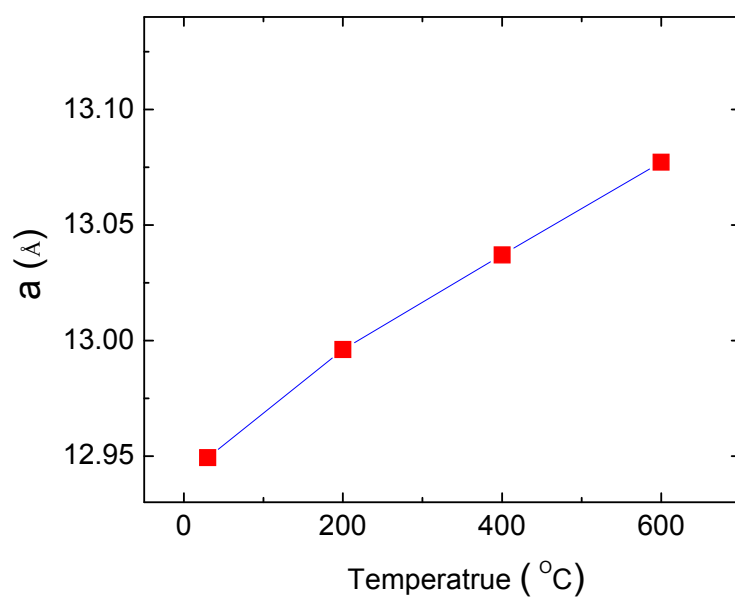


Figure S2. Lattice parameters of the garnet-tape *c*-LLZO as a function of temperature from Rietveld refinements of HTND data.

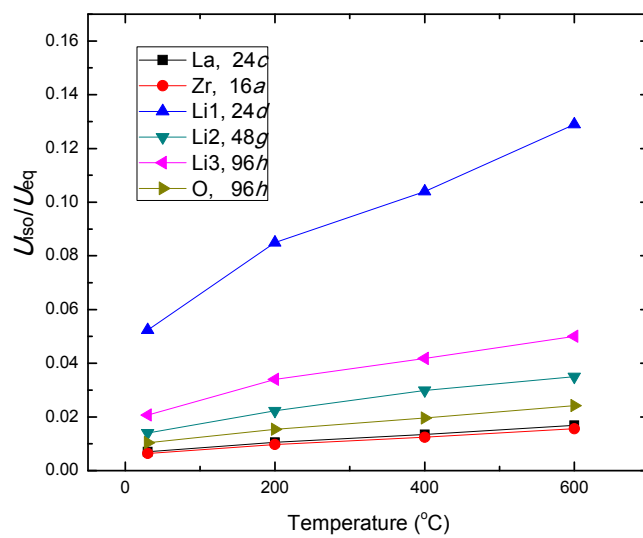


Figure S3. The anisotropic atomic displacement parameters of *c*-Li<sub>7</sub>La<sub>3</sub>Zr<sub>2</sub>O<sub>12</sub> as a function of temperature from Rietveld refinements of HTND data

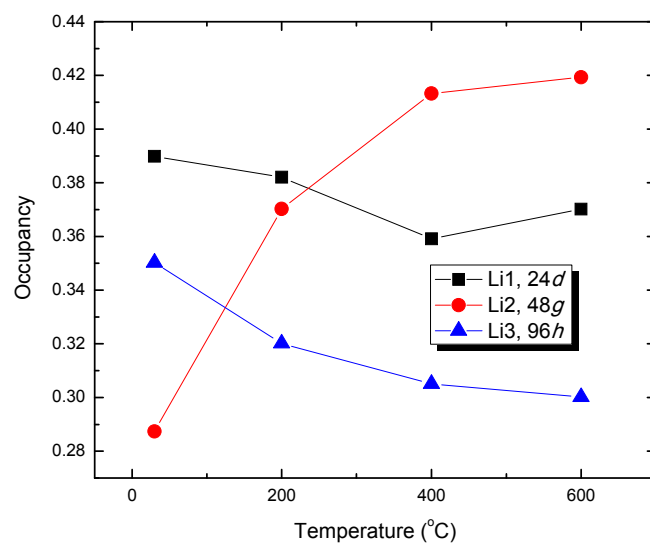


Figure S4. The occupancy of each Li site of the garnet-type *c*-LLZO as a function of temperature from Rietveld refinements of HTND data